Effects of finite aspect ratio on wind turbine airfoil measurements

2016 J. Phys.: Conf. Ser. 753 022040

(http://iopscience.iop.org/1742-6596/753/2/022040)

Effects of finite aspect ratio on wind turbine airfoil measurements

Janik Kiefer[1], Mark A Miller[1], Marcus Hultmark[1] and Martin O L Hansen[2,3]

[1] Mechanical and Aerospace Engineering, Princeton University, Princeton, New Jersey, USA
[2] DTU Wind Energy, Technical University of Denmark, Copenhagen, Denmark
[3] Andlinger Center for Energy and the Environment, Princeton University, Princeton, New Jersey, USA

E-mail: jkiefer@princeton.edu

Abstract. Wind turbines partly operate in stalled conditions within their operational cycle. To simulate these conditions, it is also necessary to obtain 2-D airfoil data in terms of lift and drag coefficients at high angles of attack. Such data has been obtained previously, but often at low aspect ratios and only barely past the stall point, where strong wall boundary layer influence is expected. In this study, the influence of the wall boundary layer on 2D airfoil data, especially in the post stall domain, is investigated. Here, a wind turbine airfoil is tested at different angles of attack and with two aspect ratios of $AR = 1$ and $AR = 2$. The tests are conducted in a wind tunnel that is pressurized up to 150 bar in order to achieve a constant Reynolds number of $Re_c = 3 \cdot 10^6$, despite the variable chord length.

1. Introduction

Even a pitch regulated wind turbine operates for some time in stalled conditions. These load cases must be included when using an aeroelastic program to prove that the structure does not fail due to ultimate or accumulated fatigue loads within the design lifetime of typically 20 years. Airfoil data are a necessary input to the Blade Element Momentum, or BEM, type algorithms most often applied in the aeroelastic programs and one must somehow obtain lift and drag at high angles of attack, either numerically or experimentally. There is a lot of uncertainty when numerically simulating stalled flow past airfoils, since the turbulence models and transition models are far from perfect for the very complicated, unsteady and three-dimensional flow. There are also many challenges when using a wind tunnel to measure 2-D lift and drag at high angles of attack and at high Reynolds numbers. In order to have a realistic Reynolds number between $Re_c = 2 \cdot 10^6 - 6 \cdot 10^6$ for a tunnel speed of 100 m/s, a chord of approximately 0.3 to 1 m is required. However, the width of the test section for such a tunnel will typically not be more than 1 to 2 m giving a maximum aspect ratio of approximately 4 for $Re_c = 3 \cdot 10^6$, and in practice often not more than $AR = 2$. In this case the boundary layer and friction from the lateral walls holding the blade section can have a severe influence on the separated low momentum flow past the airfoil at high angles of attack thus distorting the flow from what should be an infinitely long section. In this case, one is not measuring a 2-D flow past an airfoil and the walls heavily influence the lift and drag forces. To alleviate this, one may try applying boundary layer suction on the lateral walls or use compressed air to increase the momentum

near the walls, but in any case it is almost impossible to completely remove the influence of the walls. One is therefore forced to use the measured lift and drag, knowing that these are not representative of the 2-D case, or try to come up with some sort of correction, which introduces additional uncertainty. Hence, high angle of attack airfoil data are exposed to large uncertainty leading to increased safety factors in the design regulations of wind turbine blades, which in turn leads to higher than necessary costs. To quantify the influence or uncertainties committed from the lateral walls, an experimental study is proposed where the aspect ratio is varied but the Reynolds number kept constant using a unique flow facility.

2. Preceding Work

One way to obtain a high Reynolds number for measuring airfoil characteristics is to use a pressurized wind tunnel, where the density can be increased significantly. Such studies have e.g. been made by Llorenti et al [1] , Schewe [2] , Sommers and Tangler [3] and Loftin and Bursnall [4]. In [4] airfoils were tested in the NASA Langley wind tunnel up to $Re_c = 25 \cdot 10^6$, but only at an aspect ratio of 1.5 and only up to angles of attack just after $C_{l,max}$, as this study was related to airplanes. Two dedicated wind turbine airfoils with an aspect ratio of 2 were tested in [3], also in the NASA Langley Low Turbulence Pressure Tunnel and results were compared to the Eppler code with mixed success. Llorente et al [1] tested five different wind turbine specific airfoils, among them the DU 91-W2-250 from TU Delft, in the pressurized DNW-HDG wind tunnel in Göttingen and in the more conventional Low-Speed Low Turbulence Wind Tunnel at TU Delft. The AR in the DNW tunnel was 6 and in the non-pressurized LSLT Wind Tunnel the AR had to be decreased to 2 in order to maintain a similar Reynolds number. The agreement for the DU 91-W2-250 airfoil was quite good except at negative angles of attack near stall, which could perhaps be related to the different aspect ratio. The experiments in [2], which were also performed in the high pressure wind tunnel in Göttingen show a significant effect on the maximum lift even for quite high Reynolds numbers using a 27% thick airfoil. Furthermore, oil flow visualizations have shown that the distortion from the endplates is very evident. The visualizations indicate that for a Reynolds number around $Re_c = 1 \cdot 10^6$ the surface flow exhibits some large, periodic, mushroom-like structures. The wavelength of these mushroom-like structures, when compared to the chord length, may be affected by the aspect ratio. The same effect can be observed when the Reynolds number is increased up to $Re_c = 7 \cdot 10^6$. The structures disappear, but even for an aspect ratio of 6 the effect from the endplates is very visible and must affect the overall loading.

3. Experimental Setup

Forces and moments acting on the airfoil were acquired by a multi-axis load cell by *JR3*[1] with a measuring range of $\pm 1000\ N$ and an accuracy of $\pm 2.5\ N$. The load cell allows the analog data acquisition of all six degrees of freedom ($F_x, F_y, F_z . M_x, M_y\ and\ M_z$) simultaneously, which is achieved by the internal excitation of metal foil strain gages. The load signal is amplified and combined with the required excitation voltage of the strain gage bridges, which results in force and moment signals for all axes. Because multi-axis sensors tend to have a degree of cross-coupling, it is necessary to multiply the signal vector with a calibration matrix provided by the manufacturer in order to attain the correct voltages and hence the forces and moments.

A rotary table with an attached stepper motor allows the angle of attack to be varied in a range of $\alpha = 0° - 360°$. The stepper motor was programmed to make use of its micro-stepping ability, resulting in an angle resolution of $\alpha = 0.028°$. To find $\alpha = 0°$, a value of $C_l = 0.3$ obtained by the force sensor was used as a reference point for the asymmetric airfoil; referring to the values of figure 14 in [5]. All mounting components to hold the airfoil and the endplates were made out of stainless steel. The material of the airfoils is high-strength aluminum. The airfoil

[1] JR3 Multi-Axis Force-Torque Sensor, model number: 75E20A4-I125-EF-1000N

surface was polished to achieve a smooth surface finish. The spans of both airfoils are equal and therefore the mounting structures as well as the endplates maintained in the same location relative to the wind tunnel. Because the wind tunnel has a circular cross section, endplates were used to make the tests comparable to previous experiments where the airfoils were mounted flush with the plane tunnel walls.

The flow velocities were acquired with two Pitot tubes. One Pitot static probe was mounted 700 mm upstream of the airfoil to capture the undisturbed free stream velocity in a distance of 80 mm from the wall. The primary acquisition probe is a maneuverable Pitot probe on a traverse system, downstream of the airfoil. The dynamic pressure was measured with two differential pressure transducers (Validyne DP-15) with a range of ± 0.33 $psid$ to ± 0.5 $psid$ and an accuracy of $\pm 1.25 \cdot 10^{-3}$ psi over the full measuring range. A second Pitot static probe on the traverse system was used to supply the static pressure for the pressure transducer of the maneuverable Pitot probe. The traverse system allows the primary acquisition probe to be moved perpendicular to the airfoil span and flow direction as well as in a stream-wise direction to achieve the same relative downstream distance of $x/c = 3.5$ for the wake measurements, independent of the chord length of the airfoil. Figure 1 shows the experimental setup with all its components.

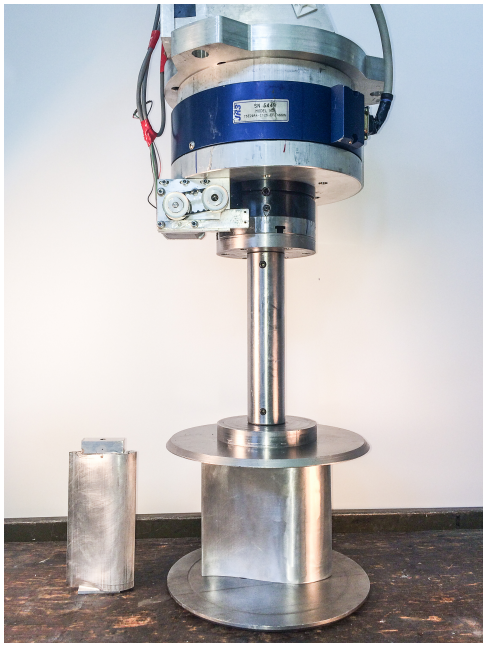

Figure 1. The experimental setup. From top to bottom: Mounting plate, force sensor in blue, rotary table with stepper motor, mounting rod, upper endplate, AR 1 - airfoil, lower endplate. AR 2 - airfoil for comparison on the left.

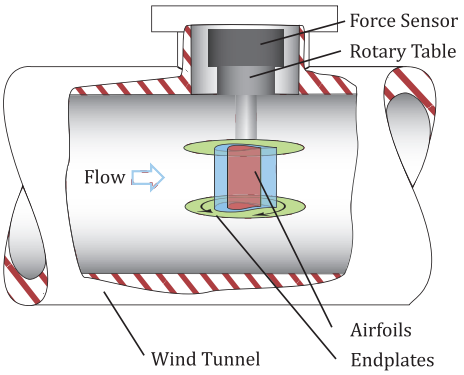

Figure 2. Schematic of the experimental setup inside the wind tunnel. The colors blue and red symbolize the airfoils in two different aspect ratios.

4. Approach & Methods

The objective of this work is to perform measurements for two aspect ratios of $AR = 1$ and $AR = 2$ for the asymmetric DU 97-W3-300 airfoil. The Reynolds number is held constant in order isolate the effect of the end-walls and draw a conclusion about the wall boundary layer influence on 2-D airfoil tests. For both aspect ratios, the dimensions of the airfoils are chosen to

maintain a wing tip deflection of less than 1% relative to span and a blockage ratio of less than 10% for all angles of attack. The end-walls are represented by endplates of a constant size for all aspect ratios. The pressurized wind tunnel, the High Reynolds number Test Facility (HRTF), is capable of adjusting the tunnel velocity from $U_\infty = 0 - 10\ m/s$ and the air density in a range of $\rho = 1.2 - 240\ kg/m^3$ or up to $p_\infty = 210\ atm$. A chord Reynolds number of $Re_c = 3 \cdot 10^6$ was achieved for the AR1-airfoil by testing at $p_\infty = 81.8\ atm$ and $U_\infty = 4.6\ m/s$. The AR2-airfoil with its shorter chord length required a higher tunnel pressure of $p_\infty = 149.1\ atm$ and a free-stream velocity of $U_\infty = 5.8\ m/s$ to maintain the same Reynolds number.

Table 1. Dimensions.

Airfoil	Chord [mm]	Span [mm]	Endplate-Ø [mm]	Tunnel–Ø [mm]	Blockage [%]
AR1	130	130	200	490	9.34
AR2	65	130	200	490	4.67

Wind tunnel corrections were applied to lift and drag data with equations found on page 179 in [6]. The equations take the airfoil shape, the airfoil size relative to the tunnel size and the Mach number into account to correct for blockage effects. Because the speed of sound is a weak function of pressure, and the velocities are kept low, testing in a pressurized facility results in low Mach numbers. For the case of $Re_c = 3 \cdot 10^6$ and $AR = 2$ The free-stream Mach number is as low as $Ma = 0.01$. Hence, any compressibility effects can be neglected even at very large Reynolds numbers.

5. Results

The C_l-curve in figure 3 illustrates the mean lift coefficient averaged over three separate runs and plotted in comparison to existing data from [5]. The curves show good agreement within the range of lower angles of attack.

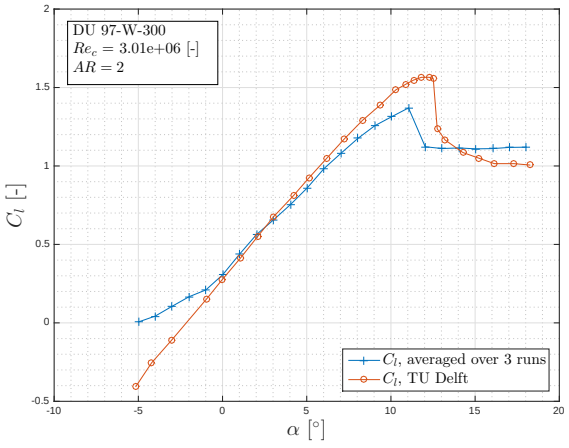

Figure 3. The averaged lift curve of three AR 2 - samples compared to data from [5]

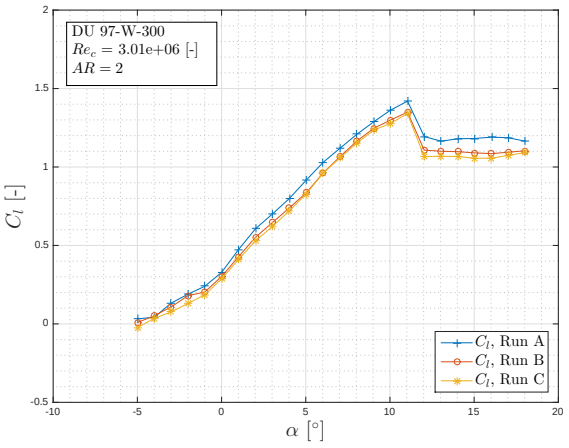

Figure 4. Repeatability of the experiment shown for $AR = 2$.

However, with increasing angles of attack the slope of the obtained lift curve slightly decreases before reaching the maximum value of $C_{l,max} = 1.37$. The decrease of lift in the post stall region

is less pronounced compared to the data of Timmer and Rooij and maintains a relatively constant value of about $C_l = 1.1$ up to $\alpha = 18°$. With decreasing angles of attack below $\alpha = 0°$ the two curves diverge. The experimental setup achieved good repeatability throughout the various runs as shown in figure 4, where three tests are shown.

The construction of the experimental setup causes the force balance to measure not only the drag of the airfoil but also the drag of the end-plates and the mounting structures. The mean velocity was measured in the wake of the airfoil at angles of attack $\alpha = -4,\ 0,\ 4°$.

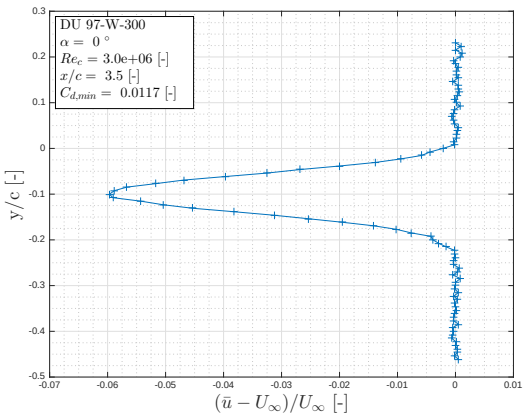

Figure 5. Velocity deficit in wake of the AR 2 - airfoil at $\alpha = 0°$.

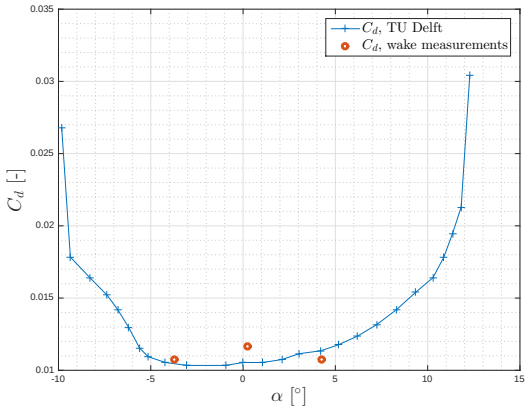

Figure 6. Drag obtained from velocity profiles of the AR 2 - airfoil at three different angles of attack, compared to drag from [5]

Figure 5 shows the measured velocity profile in the wake at a downstream distance of $x/c = 3.5$ and figure 6 shows the measured drag coefficient values in comparison to data from [5], where good agreement can be seen.

Figure 7 shows the effect of varied aspect ratio on the lift coefficients measured. Both airfoils, $AR = 1$ and $AR = 2$ were tested at a constant Reynolds number of $Re_c = 3 \cdot 10^6$.

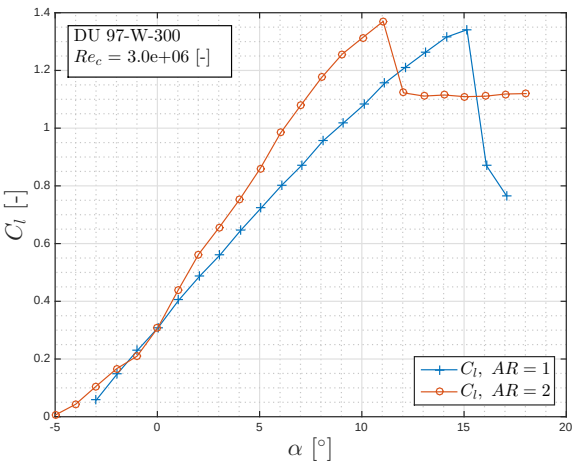

Figure 7. Comparison of lift coefficient for identical airfoils at different aspect ratios.

Each curve shown represents the mean lift coefficient values for each angle of attack from three separate tests. The most significant effect is the change in the slope of the curves. The higher aspect ratio airfoil produces a significantly steeper slope and thus a stall point at smaller angles of attack. The maximum lift value is slightly higher for the higher aspect ratio. Whereas the AR 2 - airfoil recovers within 1 degree in angle of attack from its loss in lift after the stall point, the lift of the lower aspect ratio airfoil drops to much lower values. Negative angles of attack show a potential derivation in lift between the two curves, which will be investigated in future work. Consequently, the AR 2 - airfoil shows better agreement with the data from TU Delft compared to the AR 1 - airfoil.

6. Conclusion

A significant difference in the lift curve appears to be caused by the change of the aspect ratio of an airfoil. With higher aspect ratio, the slope of the lift curves becomes steeper, the maximum lift is slightly increased, and the stall point appears much earlier. Drag measurements in the wake of the airfoil show good agreement at lower angles of attack with previously obtained data from other groups. The experimental setup is capable of testing airfoils at high angles of attack at high Reynolds numbers and furthermore demonstrates repeatability of the experiments and to previous measurements.

7. Future Work

Airfoils with higher aspect ratios need to be tested in order to draw a concrete conclusion about the encountered effect and to find guidelines for the minimal aspect ratio of airfoils for 2D tests in wind tunnels. The region of negative angles of attack and its deviation from previously published data has to be further examined. Furthermore, the test setup allows the acquisition of C_l-curves in a range of $0 - 360°$, yet with small blockage ratios, which is very interesting in coherence with computational simulations of wind turbines and their varying inflow angles.

Acknowledgments

The authors would like to thank Dan Hoffman for his relentless help with machining and realizing the technical side of the experiments. The project was partially funded by NSF CBET-1435254 (program manager Dr. Gregory Rorrer).

References

[1] Llorente et al 2014 Wind tunnel tests of wind turbine airfoils at high Reynolds numbers *J. Phys.: Conf. Series* **524** 012012
[2] Schewe G 2001 Reynolds-number effects in flow around more-or-less bluff bodies*J. Wind Eng. and Ind. Aerod. 89* 1267-1289
[3] Sommers D M and Tangler J L 2000 Wind-tunnel tests of two airfoils for wind turbines operating at high Reynolds numbers NREL/CP-500-277891
[4] Loftin L K and Bursnall W J 1948 The effects of variation in Reynolds numbers between 3.0X106 and 25.0X106 upon the aerodynamic characteristics of a number of NACA 6-series airfoil sections NACA Report 964
[5] Timmer W A and Van Rooij R P J O M 2003 Summary of the delft university wind turbine dedicated airfoils AIAA-2003-0352:11-21
[6] Allen H J and Vincenti W G 1944 Wall-interference in a two-dimensional-flow wund tunnel, with consideration of the effect of compressibility NACA Report 782